

Fluorescence excitation enhancement by Bloch surface wave in all-polymer one-dimensional photonic structure

L. Fornasari, F. Floris, M. Patrini, G. Canazza, G. Guizzetti, D. Comoretto, and F. Marabelli

Citation: [Applied Physics Letters](#) **105**, 053303 (2014); doi: 10.1063/1.4892423

View online: <http://dx.doi.org/10.1063/1.4892423>

View Table of Contents: <http://scitation.aip.org/content/aip/journal/apl/105/5?ver=pdfcov>

Published by the [AIP Publishing](#)

Articles you may be interested in

[Enhancement of two-photon excited fluorescence in two-dimensional nonlinear optical polymer photonic crystal waveguides](#)

Appl. Phys. Lett. **93**, 111110 (2008); 10.1063/1.2985902

[One-dimensional birefringent photonic crystal laser](#)

J. Appl. Phys. **103**, 033103 (2008); 10.1063/1.2838184

[Thin-film polarizer based on a one-dimensional–three-dimensional–one-dimensional photonic crystal heterostructure](#)

Appl. Phys. Lett. **91**, 123515 (2007); 10.1063/1.2789662

[Polarized laser emission from an anisotropic one-dimensional photonic crystal laser](#)

Appl. Phys. Lett. **90**, 161108 (2007); 10.1063/1.2723677

[Enhancement of two-photon excited fluorescence using one-dimensional photonic crystals](#)

Appl. Phys. Lett. **75**, 3605 (1999); 10.1063/1.125402

The advertisement features a dark blue background with three columns of text and images. The first column asks 'Frustrated by old technology?' and shows a white AFM. The second column asks 'Is your AFM dead and can't be repaired?' and shows a grey tombstone with 'RIP My Old AFM 1994-2015'. The third column asks 'Sick of bad customer support?' and shows a man with glasses shouting. To the right, a large white box contains the text 'It is time to upgrade your AFM' in orange, followed by 'Minimum \$20,000 trade-in discount for purchases before August 31st' in white. Below this, it says 'Asylum Research is today's technology leader in AFM' in orange. At the bottom right is the Oxford Instruments logo with the tagline 'The Business of Science®' and the email 'dropmyoldAFM@oxinst.com'.

Fluorescence excitation enhancement by Bloch surface wave in all-polymer one-dimensional photonic structure

L. Fornasari,¹ F. Floris,¹ M. Patrini,¹ G. Canazza,² G. Guizzetti,¹ D. Comoretto,² and F. Marabelli^{1,a)}

¹Dipartimento di Fisica, Università degli Studi di Pavia, via Bassi 6, 27100 Pavia, Italy

²Dipartimento di Chimica e Chimica Industriale, Università degli Studi di Genova, via Dodecaneso 31, 16146 Genova, Italy

(Received 20 May 2014; accepted 25 July 2014; published online 5 August 2014)

We demonstrate photoluminescence excitation enhancement in an all-polymer flexible one-dimensional photonic crystal structure capped with a fluorescent organic ultrathin film. When optical matching conditions between the excitation beam and the Bloch Surface Wave mode supported by the photonic structure are achieved, a ten times enhancement of the photoluminescence is observed. We notice that in these systems luminescence signal reinforcement is achieved by increasing the pump efficiency with no need of spectral resonance to the emission of the chosen fluorophore. All these features make these systems suitable candidates for easy, flexible, and cheap fluorescent sensing. © 2014 AIP Publishing LLC. [<http://dx.doi.org/10.1063/1.4892423>]

The manipulation of light is one of the most important aims of contemporary nanophotonics. The main focus is on the capability of nanostructures made of dielectric, metallic, and hybrid materials^{1–3} of concentrating e.m. field on length scales smaller than the diffraction limit, thus obtaining huge field intensity enhancement.^{4,5} Two approaches are reported in the literature: the first researches the highest performances through plasmonic or inorganic systems, which both require expensive and slow fabrication processes, the second is the looking for alternative systems with comparably high performances, through reliable and cheap fabrication techniques. This distinction is significant since plasmonic and photonic structure could have a high impact in many different applications (biosensing, photovoltaics, and telecommunication),^{6,7} which only become realistic if fabrication processes are easily extensible to large-scale production. Besides metal-dielectric interfaces and metallic nanostructures, another important mean to manipulate and modify light propagation is represented by Photonic Crystals (PhCs). A PhC is a dielectric structure with a spatial modulation of the dielectric function having a period of the order of the involved wavelength.⁸ In particular, a one dimensional PhC, such as a Distributed Bragg Reflector (DBR), exhibits a photonic band gap which prevents the propagation of light within a certain frequency range.

Bloch Surface Waves (BSW) are propagation modes at the surface of a DBR.^{9–11} These modes have frequency within the photonic band gap, so light cannot propagate through the periodic structure, and near-interface localization is achieved owing to total internal reflection at the surface of the bounding medium. In many aspects, BSWs can be thought of as the dielectric analogues of Surface Plasmon Polaritons¹² and should be exploited to modify the fluorescence lifetime and to spectrally and spatially reshape the fluorescence emission. Nevertheless, not many papers can be found in the literature on this subject.

A study of the radiative decay engineering of fluorescence has been recently proposed by Lakowicz *et al.*^{13,14} on inorganic DBR made of SiO₂ and Si₃N₄. However, some authors have demonstrated that high-quality DBR can be obtained using polymer materials and cheap deposition techniques.^{15–19} Polymer photonic structures are traditionally used as colour responsive materials;¹⁹ in this work, instead we propose the use of all-polymer structures to enhance and manipulate the emission of a fluorescent polymer, by exploiting a BSW excitation and envisaging an original application in sensor devices.

Cellulose acetate (CA, M_w 61 000, refractive index $n = 1.475$ at 600 nm, from Sigma Aldrich), and poly(vinyl-carbazole) (PVK, M_w 90 000, $n = 1.675$ at 600 nm, from Across Organics) have been employed to obtain high optical quality DBR by dynamic spin coating of polymer solutions in orthogonal solvents. Cellulose acetate was solved in 4-hydroxy-4-methyl-2-pentanone (diacetone alcohol, from Sigma Aldrich) with concentration about 24 g/l, while PVK was solved in toluene (Sigma Aldrich) at similar concentration. The poly(9,9-dioctylfluorenyl-2,7-diyl-co-1,4-benzo-(2,1'-3)-thiadiazole) (F8BT) was purchased from American Dye Source and its molecular mass is unknown. It was solved in toluene to obtain pure F8BT films; concentrations employed vary from 10 up to 30 g/l. All materials and solvents have been used as received without any further purification. Dynamic spin coating (Novocontrol spinner model SCV) is performed over glass substrates in laboratory environment without temperature or humidity control. Layer thickness was varied by changing the spinning speed in the range 60–150 revolutions per second (rps) and/or solution concentration. Ten period DBR structures have been prepared. After each bilayer deposition, a 4 min baking step at 70 °C on a hot plate was performed in order to improve the optical quality of the films.²⁰ Finally, a thin F8BT (the fluorescent active medium) film is cast on top of the DBR structure terminated by a CA layer.

In order to determine the film thickness—thus calibrating deposition parameters—and to characterize the dielectric

^{a)} Author to whom correspondence should be addressed. Electronic mail: franco.marabelli@unipv.it.

response of each material, thin films of each single polymer as well as suitable bilayers have been spin-cast on glass substrates in the same experimental conditions as for the DBR growth. Spectroscopic ellipsometry in the 0.25–2.5 μm range were measured by a VASE instrument by J.A. Woollam Co., Inc., at different angles of incidence from 60° to 75°. Modelling of the complex dielectric function $\varepsilon = \varepsilon_1 + i\varepsilon_2$ of CA, PVK, and F8BT thin films was implemented through oscillator models, which guarantee Kramers-Kronig consistency and do give results in general agreement to the available literature data.^{20–22} Typical thicknesses of CA, PVK, and F8BT layers were found to be 65 nm, 120 nm, and 3 nm, respectively.

The full optical characterization of single polymer films, bilayers (PVK and F8BT on CA), as well as DBRs, has been performed by transmittance, attenuated total reflectance (ATR), spectroscopic ellipsometry (SE), and photoluminescence (PL) measurements. In order to perform angle-resolved ATR measurements, a Poly(methyl methacrylate) (PMMA) semicylinder has been glued to the polymer DBR substrates and used as a prism for white light probing, through a Fourier Transform Infrared spectrometer coupled to a home-made micro-reflectance/luminescence setup in Kretschmann configuration.²³ Reference measurements with a bare PMMA prism and a glass substrate glued onto the prism have been also performed in order to check for spurious contributions to the ATR spectra as well as to normalize the angle dependent DBR reflectance spectra. PL pumping was obtained with a diode laser beam (405 nm, 5 mW output power) impinging on the sample from the back, using the same prism configuration used for ATR. The emission beam was collected by a lens in front of the sample, with an acceptance angle of about 10°. Numerical simulation of all ATR spectra has been performed with WVASE32[®] software, by using the dielectric function dispersion and film thicknesses previously determined.

As a first step, we performed an ATR characterization of the bare polymer DBR (i.e., without the F8BT capping layer). The normalized reflectance spectra as a function of the incident angle for *s*-polarization are shown in Fig. 1 (solid lines). The dispersion of the 1st order photonic band gap feature (the strong reflectance peak) as a function of the incidence angle is evident. Interference fringes also appear due to the finite size of the whole CA-PVK multilayer and the refractive index contrast between this last and the substrate. Such fringes are very sensitive to the whole thickness of the system and to the optical quality of the structure. Moreover, spectral position, intensity, and width of the reflectance peak associated to the photonic band gap depend on the dielectric contrast and the thickness of the CA and PVK layers as well as on the number of periods. In the present case, the DBR structure was designed with a band gap center wavelength at about $\lambda = 580\text{ nm}$ at normal incidence and with an angular dispersion allowing to match at about 40° of incidence the F8BT absorption spectrum (below $\lambda = 500\text{ nm}$). Above the critical angle of the system in air—around 43°—the reflectance spectrum achieves the ATR regime and the optical response of the DBR is almost the same as that of the PMMA prism, which is used to normalize the DBR spectra.

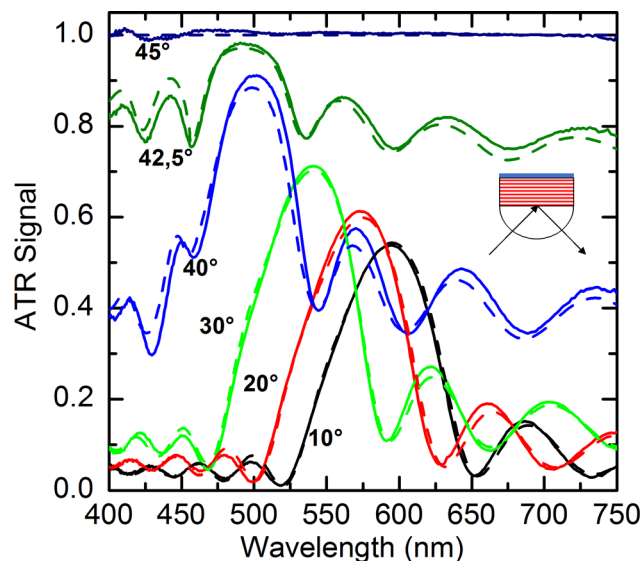


FIG. 1. Variable-angle *s*-polarized ATR spectra of a bare CA/PVK DBR structure as a function of the incident angle, as measured in Kretschmann configuration (full lines) and simulated (dashed lines). The scheme of the optical geometry is shown in the inset (not in scale).

In Fig. 1, we also report the results of modelling the optical response of the DBR (dashed lines). Simulation has been performed by using the optical functions derived by the simultaneous analysis of the transmittance and SE spectra of single films, while the thickness of CA and PVK layers were free parameters. The best-fit thicknesses to the ATR experimental curves very well agree with the ones independently obtained by the analysis of the transmittance and SE spectra of the DBR. In a refinement step, also the angle of incidence has been slightly adjusted (about 1°), i.e., within the experimental uncertainty. The agreement confirms the high quality of films and interfaces of the polymer DBR structure.

Casting the active layer on top of the DBR structure, the F8BT absorbance band is observed in transmittance²⁰ and SE spectra around 400–500 nm wavelengths. Actually, no relevant changes are detected in reflectance spectra below the critical angle. Conversely, at the threshold of the ATR regime (43°), the ATR response is strongly modified, as shown in Fig. 2. While for the bare DBR at similar incidence angle, the optical response is dominated by total reflection, when F8BT film is on top of DBR, two absorption like, angle-dependent features appear in the spectra. One is the group of structures between 450 and 500 nm in the ATR spectra of Fig. 2. This is due to the interplay of the absorption of F8BT (which tends to lower the reflectance value) with the onset of the band gap structure (which tends to hinder light propagation, and then absorbance, through the DBR).

Then, a second relatively narrow feature emerges near the high energy edge of—but within—the bandgap, from 450 to 400 nm, in the spectra and exhibits a clear dispersion behavior with the incidence angle. We will focus on this feature (hereafter named BSW). In fact, it is not related to absorption of F8BT and it does not appear in *p*-polarized reflectance spectra at any angle of incidence.^{9,24} Simulations very well reproduce the experimental curves, as reported in Fig. 2(b), thus allowing us to investigate the BSW

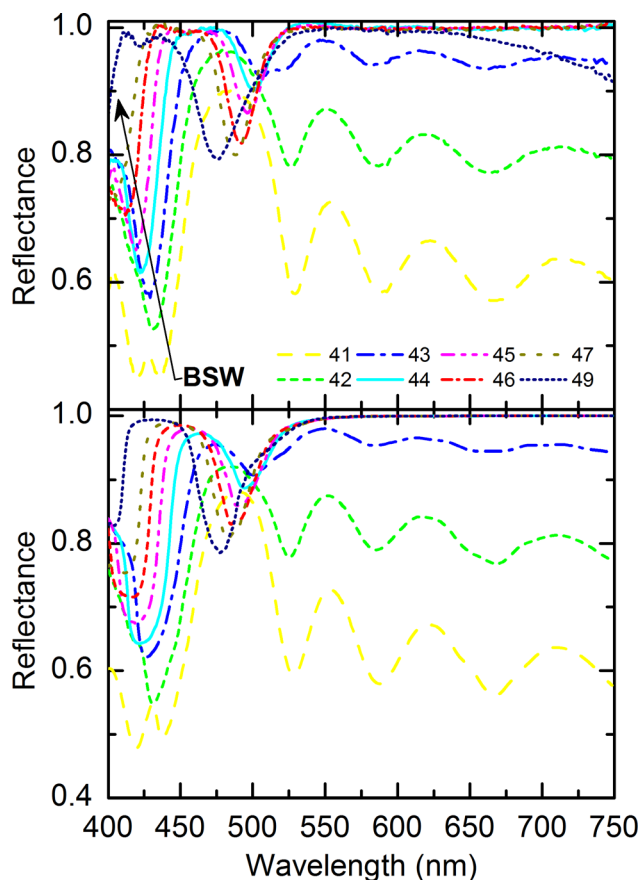


FIG. 2. (a) *s*-polarized ATR spectra as a function of the incident angle for a DBR covered by a F8BT thin film in the ATR regime; (b) the same from simulation.

dependence on the structural parameters. By varying structural parameters in the simulation, we noticed that:

- the BSW wavelength and its angular dispersion are strongly dependent on the thickness of the CA and PVK layers composing the DBR;
- increasing the number of DBR periods (i) the BSW wavelength is un-changed, (ii) its intensity slightly increases, and (iii) its linewidth becomes vanishingly small.

Then, the BSW structure is strictly related to the DBR band gap. Nevertheless, when the conditions for the total reflection are modified, e.g., by increasing the refractive index of the medium above the F8BT film, the structures related to band gap and absorption (the ones between 450 and 500 nm in Fig. 2) remain, whereas the BSW feature we are focusing disappears. Upon increasing the thickness of the active F8BT layer from 1 nm up to 5 nm (experimentally we explored the range 2–3 nm), the intensity of the BSW feature increases. Notice that the thickness variation does not affect the DBR optical response or the ATR regime. Then, BSW is strongly affected by the properties of the last layer and seems localized there.

All these evidences point out to assign the BSW feature appearing between 400 and 450 nm to a Bloch Surface Wave running through the last layer of the capped DBR structure.²⁰ When suitable photon polarization, energy and wavevector (incidence angle) matching is attained, the BSW mode can be excited by the impinging radiation. Since the fluorescent

and absorbing layer is cast on the surface, the excitation of the BSW mode is observed as a dip in the reflectance spectrum. The relatively large spectral width of the BSW fingerprint as compared to that observed in high refractive index contrast inorganic counterparts¹⁰ is due to finite size effects of the one-dimensional photonic structure.

The e.m. field spatial localization associated to the BSW mode can be exploited to enhance the pumping efficiency in a fluorescence experiment. While some result has been reported on the confinement of the emitted (fluorescent) field,^{14,15} still few works are related to excitation field confinement. We measured the PL spectrum of our all-polymer DBR capped with the F8BT thin film as a function of the incidence angle of the exciting laser beam. In order to evaluate the intensity enhancement caused by the BSW excitation, we used suitable reference structures, i.e., F8BT films on a glass substrate either free or glued on a PMMA prism. The thickness of the active layer was the same as that cast on top of the DBR structure.

As expected with an *s*-polarized laser beam input, the free film emission slowly decreases on increasing the pump incidence angle. However, it is interesting to compare (Figure 3) the emission intensity as a function of wavelength and incidence angle of the pump for the bare F8BT film (a) and the same film on top of the DBR structure (b), when both are mounted on the prism. All the spectra were normalized to the largest peak emission intensity of each series. Within each series the spectral shape is practically unchanged; nevertheless, a spectral redistribution of PL is evident between the two cases. Maximum occurs around $\lambda = 540$ nm for the bare film and 570 nm for the film on DBR; the PL bandwidth when F8BT film is on the top of the DBR is much sharper than in the PL spectrum of a bare F8BT film. The dependence on pump angle of incidence is also very different (profiles are plotted on the right of each panel of Fig. 3). For bare F8BT, PL slowly increases to the maximum approaching the critical angle of total reflection (around 43°). In the case of DBR structures, a steep signal increase occurs up to about 47°, i.e., beyond the critical angle. Then, for larger angles, the emission falls to almost zero at about 58° and then the signal recovers again to weak but not negligible values. Notice that the same incidence angles of 47° is almost exactly the one where ATR spectra in Figure 2 exhibit the BSW resonance at the wavelength of the pump laser, 405 nm. This coincidence further supports our assignment of the BSW structure to a Bloch Surface Wave excitation. For larger angles, the PhC bandgap region—due to angular dispersion—overlaps the pump frequency, and consequently, the PL signal is expected to disappear as indeed observed. Above 60°, when the lower band-edge is crossing over 405 nm, PL is excited again and its spectrum is modulated by the interference fringes of the reflectance spectrum of the DBR.

The enhancement effects associated to the spectral redistribution of the PL signal can be now pointed out. Figure 4 reports the PL spectra of the F8BT on DBR sample and of the references previously discussed. For each case, the strongest intensity spectrum has been chosen: the angle of incidence was about 30° for the bare F8BT film, 45° when on the prism, and 47° when on the DBR and prism. The F8BT PL spectrum

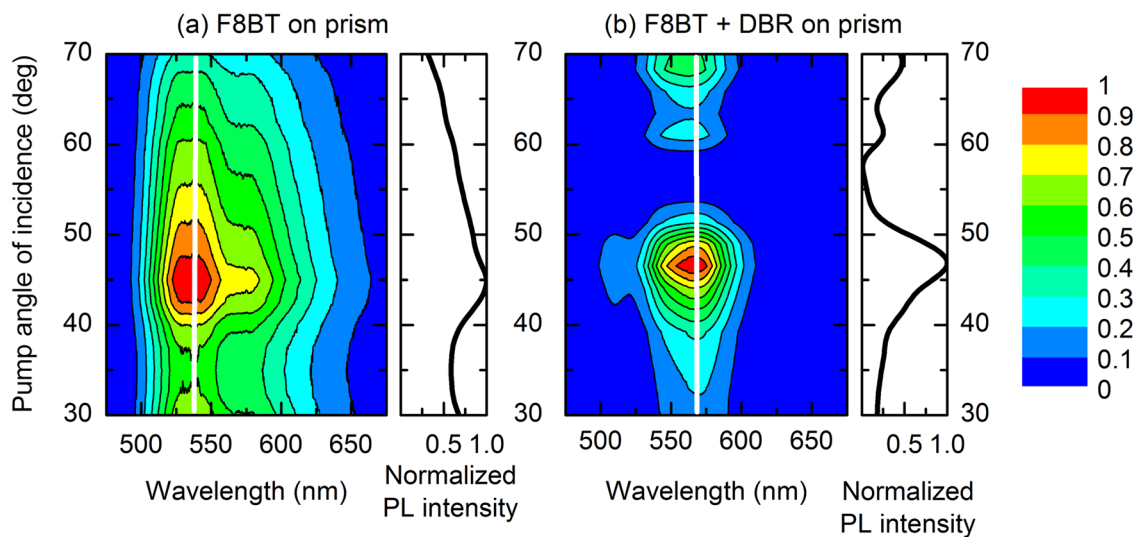


FIG. 3. F8BT photoluminescence spectral intensity maps as a function of the incident angle for a F8BT film (left) and for F8BT capping a DBR structure (right). The PL signal intensity trend at the maximum emission intensity wavelength (indicated by the white, vertical line) is shown on the right of each map.

is similar to those previously reported^{15,16} even though some structuring (530 and 580 nm) is here more evident, probably due to the ultra-low thickness of the investigated film. The use of the prism improves the PL efficiency by doubling the signal intensity. This effect can be ascribed to total reflection: light cannot escape from the surface and interaction with the material is significantly increased. Anyway, the spectral shape of PL remains unchanged.

On the contrary, the introduction of DBR causes a dramatic spectral and intensity change of the PL signal. The main peak is shifted to $\lambda = 570$ nm, while the two weak satellites at 515 and 650 nm are modulations induced by photonic band gap edges.¹⁵ The spectral shift is likely to be attributed to the interaction of the emitted light with the underlying photonic structure, which is selectively reflecting the different spectral components. Moreover, PL shows a remarkable enhancement with respect to the bare F8BT film either in terms of

intensity—a factor of ten (six if one considers peaks at different wavelengths)—or in terms of integrated signal over the whole emission spectrum (more than four times). Such an enhancement is substantially observed also with respect to F8BT on the prism (a factor of 2.5 on both quantities). We assign such an enhancement effect to the localization of the pump beam in the F8BT layer mediated by the BSW mode, which improves the photon absorption probability, and consequently increases the PL photon density.

We would notice that both angular dispersion and signal enhancement can be nicely exploited when this kind of DBRs are adopted in a sensing device. Indeed, PL signal enhancement allows to improve the sensitivity of the detection. This potential could be of strong and particular interest when chemical species under investigation do not possess a specific chemical receptor group like in the case of explosives.^{25,26} In conclusion, we reported on PL enhancement via BSW excitation in all-polymer DBR capped with a fluorescent semiconducting polymer. The enhancement effect is due to the localization of the excitation beam into the fluorescent layer, which dictates very strong geometrical constraints in order to observe the effect itself. We envisaged on the possible use of such effect for sensors, in particular, for analytes without a specific chemical receptor group.

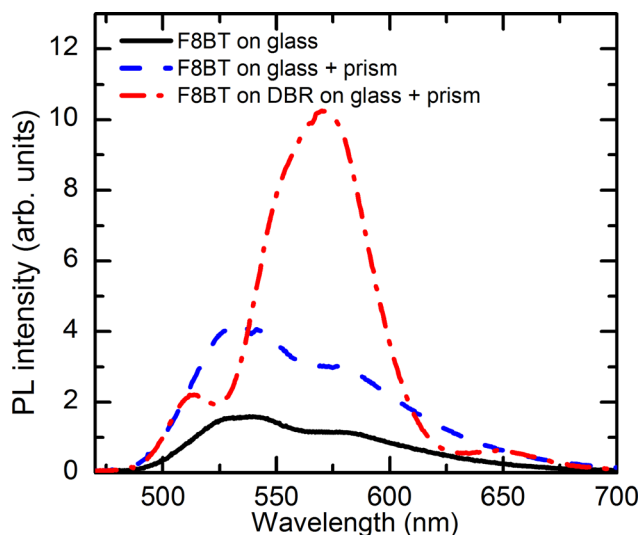


FIG. 4. Photoluminescence spectra of F8BT film on a glass slide, on a glass slide glued to a prism and on top of the DBR on the prism. Excitation was obtained with a 405 nm laser impinging from the back with *s*-polarization at incidence angle of 30°, 45°, and 47°, respectively.

The work has been mainly supported by Cariplo Foundation under the Project PHOENICS (No. 2009-2461). Work in Genova has been partially supported by the MIUR Ministry through the PRIN 2010–2011 Project (No. 2010XLLNM3).

¹R. F. Oulton, V. J. Sorger, D. A. Genov, D. F. P. Pile, and X. Zhang, *Nat. Photonics* **2**, 496–500 (2008).

²S. G. Romanov, A. V. Korovin, A. Regensburger, and U. Peschel, *Adv. Mat.* **23**, 2515–2533 (2011).

³X. Yang, A. Ishikawa, X. Yin, and X. Zhang, *ACS Nano* **5**, 2831–2838 (2011).

⁴D. K. Gramotnev and S. I. Bozhevolnyi, *Nat. Photonics* **4**, 83–91 (2010).

⁵J. A. Schuller, E. S. Barnard, W. Cai, Y. C. Jun, J. S. White, and M. L. Brongersma, *Nat. Mater.* **9**, 193–204 (2010).

⁶M. E. Stewart, C. R. Anderton, L. B. Thompson, J. Maria, S. K. Gray, J. A. Rogers, and R. G. Nuzzo, *Chem. Rev.* **108**, 494–521 (2008).

- ⁷K. M. Mayer and J. H. Hafner, *Chem. Rev.* **111**, 3828–3857 (2011).
- ⁸E. Yablonovitch, *Phys. Rev. Lett.* **58**, 2059–2062 (1987).
- ⁹M. Liscidini and J. E. Sipe, *J. Opt. Soc. Am. B: Opt. Phys.* **26**, 279–289 (2009).
- ¹⁰M. Liscidini, M. Galli, M. Patrini, R. W. Loo, M. C. Goh, C. Ricciardi, F. Giorgis, and J. E. Sipe, *Appl. Phys. Lett.* **94**, 043117 (2009).
- ¹¹S. Pirota, M. Patrini, M. Liscidini, M. Galli, G. Dacarro, G. Canazza, G. Guizzetti, D. Comoretto, and D. Bajoni, *Appl. Phys. Lett.* **104**, 051111 (2014).
- ¹²A. Yariv and P. Yeh, *Optical Waves in Crystals* (Wiley, 2002).
- ¹³R. Badugu, K. Nowaczyk, E. Descrovi, and J. R. Lakowicz, *Anal. Biochem.* **442**, 83–96 (2013).
- ¹⁴L. Han, D. Zhang, Y. Chen, R. Wang, L. Zhu, P. Wang, H. Ming, R. Badugu, and J. R. Lakowicz, *Appl. Phys. Lett.* **104**, 061115 (2014).
- ¹⁵L. Frezza, M. Patrini, M. Liscidini, and D. Comoretto, *J. Phys. Chem. C* **115**, 19939 (2011).
- ¹⁶G. Canazza, F. Scotognella, G. Lanzani, S. De Silvestri, M. Zavelani-Rossi, and D. Comoretto, *Laser Phys. Lett.* **11**, 035804 (2014).
- ¹⁷V. M. Menon, M. Luberto, N. V. Valappil, and S. Chatterjee, *Opt. Express* **16**, 19535 (2008).
- ¹⁸L. M. Goldenberg, V. Lisinetskii, and S. Schrader, *Laser Phys. Lett.* **10**, 055808 (2013).
- ¹⁹J.-H. Lee, C. Y. Koh, J. P. Singer, S. Jeon, M. Maldovan, O. Stein, and E. L. Thomas, *Adv. Mater.* **26**, 532 (2014).
- ²⁰See supplementary material at <http://dx.doi.org/10.1063/1.4892423> for data on sample quality, Abbe's number, transmittance spectra, and BSW dispersion.
- ²¹M. Campoy-Quiles, J. Nelson, P. G. Etchegoin, D. D. C. Bradley, V. Zhokhavets, G. Gobsch, H. Vaughan, A. Monkman, O. Ingänas, N. K. Persson, H. Arwin, M. Garriga, M. I. Alonso, G. Herrmann, M. Becker, W. Scholdei, M. Jahja, and C. Bubeck, *Phys. Status Solidi C* **5**, 1270–1273 (2008).
- ²²M. Campoy-Quiles, G. Heliotis, R. Xia, M. Ariu, M. Pintani, P. Etchegoin, and D. D. C. Bradley, *Adv. Funct. Mater.* **15**, 925–933 (2005).
- ²³M. Galli, D. Bajoni, M. Patrini, G. Guizzetti, D. Gerace, L. C. Andreani, M. Belotti, and Y. Chen, *Phys. Rev. B* **72**, 125322 (2005).
- ²⁴E. Descrovi, T. Sfez, M. Quaglio, D. Brunazzo, L. Dominici, F. Michelotti, H. P. Herzig, O. J. F. Martin, and F. Giorgis, *Nano Lett.* **10**, 2087–2091 (2010).
- ²⁵S. W. Thomas III, J. P. Amara, R. E. Bjork, and T. M. Swager, *Chem. Commun.* **2005**, 4572–4574.
- ²⁶A. Abboto, D. Comoretto, F. Gagliardi, and F. Marabelli, “Nuovi composti otticamente sensibili ai composti elettron-poveri,” patent application IT2012MI00636 (17 April 2012).